



Deliverable 4.6

Final models for growth

Version 2.0

WP 4
Deliverable 4.6
Lead Beneficiary: HCMR
Call identifier:
Biological and Medical Sciences - Advanced Communities: Research infrastructures in aquaculture
Topic: INFRAIA-01-2018-2019
Grant Agreement No: 871108
Dissemination level: Public
Date: 31.10.2024



This project has received funding from the European Union's Horizon 2020 research and innovation programme under grant agreement No. 871108 (AQUAEXCEL3.0). This output reflects only the author's view and the European Commission cannot be held responsible for any use that may be made of the information contained therein.

Contents

Objective	2
Background	3
Methodology.....	4
Model description.....	4
Model refinements	5
Inclusion of new species	7
Results and Discussion.....	8
Model refinements	8
Inclusion of new species	13
Conclusion.....	16
Appendix	17
References	19
Document Information	25

Objective

This document is part of the AQUAEXCEL3.0 project, *WP4 'Technological tools for improved experimental procedures'* which aims to develop a virtual laboratory system, comprising of an array of mathematical models (fish growth, hydrodynamic flow field, water quality, behavioural) that enables virtual experiments in aquaculture research facilities. This report relates to the fish growth component of the system, which is the bioenergetic model AquaFishDEB. The model captures the effects of feeding level, feed composition, feeding schedule and water characteristics on individual growth, feed consumption, waste production (faecal and non-faecal nitrogen loss, faecal dry matter, CO₂), and oxygen consumption for different species. The model includes a digestion module and has been developed and validated for several fish species. Earlier versions of the model including the prototype and the incorporation of the digestion module have been presented in detail in previous deliverables (AQUAEXCEL2020, D5.6) which also contain complete descriptions of the modelling framework, the data used, and the parametrization and validation processes.

Within AQUAEXCEL3.0, the objective was to expand the capabilities of the AquaFishDEB model and add functionalities. Namely, these include the parametrization of the model for two new species (the European sea bass and the pikeperch), further testing and validation, refinements of the digestion module including the addition of predictions for body composition and finally, the modelling of swimming effects on metabolism. The deliverable resulting from this work (D4.6 'Final models for growth') is the code containing these modifications which is provided as part of the FMU (Functional Mock-up Units) and also in standalone matlab files. This document is an accompanying file for this code, aiming to further assist user orientation. Specifically, it contains background information for the modelling framework, it describes the improvements, updates, and added functionalities that have been implemented and provides selected examples of model outputs.

Background

The AquaFishDEB model is based on the Dynamic Energy Budget theory (DEB), a qualitative and quantitative framework to study individual metabolism throughout the entire life cycle of an organism making explicit use of energy and mass balances (Kooijman, 2010). Its ability to model the bioenergetics of organisms as a function of temperature and food quantity and quality throughout their life cycle has established the DEB theory as a widely applicable approach to study fish metabolism on both wild populations and farmed fish (e.g., Pecquerie *et al.*, 2009; Serpa *et al.*, 2013; Fore *et al.*, 2016; Sadoul *et al.*, 2019; Sarà *et al.*, 2018). DEB theory describes the interconnections among the processes of assimilation, maintenance, development, growth, and reproduction of an organism throughout all stages of its life cycle, and in a dynamic environment. The AquaFishDEB model captures the effects of feed quality, feeding schedule and water characteristics on individual growth, feed consumption, waste production (faecal and non-faecal nitrogen loss, faecal dry matter) as well as gaseous exchange (oxygen consumption, carbon dioxide production) and body composition for different species.

This document describes the updates implemented in the final version of the code delivered for the AquaFishDEB model. It builds on the report D5.6 (Lika *et al.*, 2020) which described the DEB model framework on which the AquaFishDEB was based, the input/outputs of the model, the development of a new module, modelling the assimilation-digestion of food, and the methodology to estimate and calculate parameters. It also contained the parameterization of the AquaFishDEB model for three species, the gilthead seabream, the rainbow trout, and the Atlantic salmon as well as the performance, the validation, and the sensitivity of the model. Within AE3.0 an aim is to extend the model to other species, improve the existing model, and add functionality. Specifically, we have developed DEB models for two additional species, the E. sea bass (*Dicentrarchus labrax*) and the pikeperch (*Zander lucioperca*). The E. sea bass is among the most established commercial species in Mediterranean aquaculture while pikeperch is at the early stages of domestication and its farming is performed semi-intensively in ponds, often in polyculture with other species. Due to the complex trophic interactions at the pond level, the pikeperch model has been developed as a stand-alone model while the one for E. sea bass has been integrated into the virtual laboratories. Model improvements have been implemented for all species, mainly via the calibration of the digestion module with targeted nutritional data. Finally, new functionalities have been added to the AquaFishDEB, namely the inclusion of predictions for body composition as well as the explicit modelling of the effects of swimming on fish metabolism.

Methodology

The section contains a brief description of the AquaFishDEB model and its main structure. Furthermore, it describes the methodology used for the inclusion of two new species, the pikeperch and the *E. seabass* model, as well as refinements on the digestion module including the addition of body composition predictions. Finally, it describes the process for modelling the energetic costs of swimming.

Model description

The AquaFishDEB model is the end product of a two-step modelling procedure. The first step involves the development and parameterisation of the DEB model which describes the dynamics of an individual fish of a given species. In the second step, these parameters are fed to the AquaFishDEB model that simulates the dynamics for a group of fish exposed to specified rearing conditions. Variables of interest for aquaculture researchers can then be obtained such as growth (e.g., weight-at-time, biomass of the population), feeding characteristics (e.g., feed intake, feed conversion ratio) as well as waste production (faecal and non-faecal nitrogenous loss) and gaseous exchange (O_2 consumption and CO_2 production).

Regarding the structure of the DEB model, the state of an individual fish is described by four variables: volume of structural mass V , energy reserve E , energy invested to maturation E_H , and energy invested to reproduction E_R (for adults). An individual fish converts food to reserves (a process called assimilation) and allocates mobilized reserves to somatic and maturity maintenance, growth (i.e., increase in structural body mass) and maturation/reproduction. Food uptake depends on food availability and fish size. Food is converted into reserves with a constant efficiency, which is specific to feed quality. A fixed fraction κ of the mobilized energy is used for somatic functions, such as somatic maintenance and growth, while the remaining $1-\kappa$ fraction is allocated to maturation/reproduction, after subtraction of maturity maintenance costs. In addition, a digestion-assimilation module is incorporated in the AquaFishDEB to model the food, M_x , dynamics in the gut and the process of assimilation of the food from the gut wall. This module, accounts for the proximate composition of the food, follows the differential digestion of its various macronutrients (proteins, lipids, carbohydrates) for the formation of reserves and allows the explicit monitoring of gut contents and nitrogenous waste under various feeding regimes (feeding level, composition, feeding schedule). Model equations and parameters are summarized in Tables A1-A3 in the Appendix. For a more comprehensive description of the DEB theory and a full list of the equations and the nomenclature used we refer to, see Kooijman (2010) and Stavrakidis-Zachou et al., (2019) as well as D5.6 (Lika et al., 2020) for the derivation of the digestion module.

Model refinements

Improving the digestion module

The digestion module describes the rates at which the ingested food is digested and assimilated into reserves. For AquaFishDEB, we do not explicitly model the ingestion process, but rather assume that at the time of feeding, food is instantaneously transferred to the stomach. The amount that is consumed is however constrained by the physical properties of the stomach, specifically stomach volume. We here assume stomach volume (V_g) to be proportional to the structural volume of the fish via the shape coefficient δ_g : $V_g = \delta_g V$. Once ingested, food is processed by enzymes and broken down to form products that will then be absorbed through the digestive wall and form the reserve molecules. The rate at which the products are generated by the digestion process is proportional to the digestive surface area and the mass of food, M_X (in mol), in the stomach (Helander and Fändriks, 2014). This rate therefore is noted as $\dot{J}_d = \{J_{Xgm}\}L^2M_X$, where $\{J_{Xgm}\}$ is the maximum surface-area-specific rate of digestion and L the structural length, a metric for the size of the individual. Subsequently, we model the absorption of the products, which we distinguish between protein (X_P) and non-protein (X_{nP}), through the digestive wall and the transformation into reserves (assimilation process) using the synthesizing unit (SU) concept of DEB theory (Kooijman, 2010). The SUs are generalized enzymes that bind and process one or more substrates to form one or more products. In this case, the two complementary substrates (protein and non-protein) are processed in parallel to produce the generalized reserves, E . The rate of reserve formation or assimilation rate is $\dot{J}_{EA} = \{J_{EAm}\}f_XL^2$ where f_X represents the scaled functional response for digestion and $\{J_{EAm}\}$ is the maximum surface-specific assimilation (Table A1).

It is evident from the above, that the application of the digestion module requires the estimation of additional species-specific parameters like the shape coefficient for the stomach and the surface-area-specific maximum digestion and assimilation rates. To accomplish this, we relied on published experimental data. Specifically, data were gathered on gastric evacuation for various temperatures and fish sizes, as well as data on stomach volume as a function of fish size. Examples of model fitting are shown in results.

Body composition

The final version of AquaFishDEB incorporates predictions for the body composition of the fish. Typically, the wet weight of the fish consists of more than 95% water ('moisture'), proteins, and lipids as well as small amounts of inorganic compounds ('ash') and negligible contributions from carbohydrates (Breck, 2014; Silva *et al.*, 2015), which we here exclude from the formulations for simplicity. In the DEB framework, the total biomass of an organism is the sum of the mass of structure and reserves: $M = M_V + M_E$ (in mol). Structure and reserves are both generalized compounds of constant chemical composition with their composition being expressed as the relative abundance of hydrogen (H), oxygen (O), and nitrogen (N) to carbon (C). Thus, for example, a molecule of reserve has the formula $CH_{n_{HE}}O_{n_{OE}}N_{n_{NE}}$, where n_{*E} are the chemical indices, e.g. n_{NE} represents the molar N:C ratio of reserve. Each generalized compound has specified chemical potential (μ_*), specific density (d_*), and molecular weight (w_*). Therefore, by multiplying the components of the fish biomass with the wet and dry molecular weights of reserve and structure, respectively, the

wet ($W_w = w_{Vw}M_V + w_{Ew}M_E$) and dry ($W_d = w_{Vd}M_V + w_{Ed}M_E$) weight of the fish can be calculated. The moisture content of biomass can then be calculated from the difference between wet and dry weight.

Using the same rationale, the amount of a compound such as protein or lipids in fish biomass is the sum of the compound in both the structure and reserves. While the macronutrient composition of reserve and structure remains constant over time, their relative abundance will vary depending on rearing conditions, leading to differences in body composition. To simulate these changes, the macronutrient composition of structure and reserve needs to be known. We define θ_{PrV} and θ_{LV} the fraction of protein and lipid in structural biomass and the respective fractions θ_{PrE} and θ_{LE} in reserve. Assuming that an egg consists approximately only of reserve and that a sufficiently starved individual has depleted its reserves and consists only of structure, the above aforementioned fractions can be estimated from relevant data. This approach allows for the approximate calculation of these fractions based on observations of individuals at these physiological extremes. Specifically, here we used the proximate composition of eggs and the whole-body composition of fish in starvation trials: Rennie *et al.* (2005) for Atlantic salmon, Washburn *et al.* (1990) for rainbow trout, Fernández-Palacios *et al.* (1997) for gilthead seabream and Cerdá *et al.* (1994) for E. seabass.

Modeling the cost of swimming

An organism must perform energy-demanding processes in order to maintain the functionality of its vital systems and therefore remain alive. These energetic costs are known as maintenance costs and the aforementioned processes include, amongst others, the maintenance of concentration gradients across membranes, a basal cost of movement, the turnover of structural body proteins and the continuous production of scales, and epithelial cells. Since these processes are performed at a cellular level, the assumption that the basic maintenance costs are proportional to the volume of the organism is rather straightforward, and it is the one adopted by the DEB framework. Therefore, during the development of the AquaFishDEB model, we have modelled somatic maintenance (\dot{p}_s) as proportional to the structural volume (V) and dependent on a species-specific parameter, the volume specific somatic maintenance rate ($[\dot{p}_M]$, $\text{J d}^{-1} \text{cm}^{-3}$)

$$\dot{p}_s = [\dot{p}_M]V$$

Swimming is an energetically costly activity since any movement differential to that of water requires the production of thrust to overcome drag forces. While there are many factors affecting the total costs of swimming, these costs are positively correlated primarily with two factors: swimming speed and the fish size. This is because drag increases with increasing swimming speed as well as the surface of the frontal area of the fish (Ohlberger *et al.*, 2005). In fact, respirometry shows that swimming costs, as indirectly measured via oxygen consumption, increase exponentially with swimming speed (Hejlesen *et al.*, 2024; Hvas and Oppedal, 2019), while the capacity for oxygen acquisition, which is crucial for sustaining swimming, is dependent on the surface area of the gills which deliver oxygen to the bloodstream, and the ventilation rate (Pörtner *et al.*, 2017). Moreover, drag is highly dependent on the morphology of the fish. In particular, the shape of certain species is more streamline than others, allowing them to reduce the drag and therefore the overall costs of locomotion.

Based on the above, we here incorporate the metabolic cost of swimming as an additional cost to the somatic maintenance costs described below. This additional term assumes that the swimming costs are proportional to the surface area of the fish and depend on the swimming speed of the fish compared to a reference baseline value (v_{ref}) as well as species specific parameter accounting for morphological traits, the surface specific cost for locomotion ($\{\dot{p}_L\}$, J d⁻¹ cm²). Thus, the somatic maintenance rate is given by

$$\dot{p}_s = [\dot{p}_M]V + \{\dot{p}_L\} \left(\frac{v}{v_{ref}} \right)^2 V^{2/3}$$

For each of the species, respirometry data under increasing swimming speeds were obtained from literature for the parametrization of this function.

Inclusion of new species

The DEB parameters can be estimated as described in Marques *et al.* (2019) and Stavrakidis-Zachou *et al.* (2019), using the freely downloadable DEBtool software (<http://www.bio.vu.nl/thb/deb/deblab/>) and a number of zero- and uni-variate data sets. For the pikeperch, parameters were estimated using data obtained from the literature and from partners of the AQUAEXCEL3.0 project. For *E. seabass*, the main DEB parameters were taken from previous parametrization of the species (Stavrakidis-Zachou *et al.*, 2019). The add-on digestion module for digestion was then calibrated using additional data relating to gastric evacuation. Subsequently the model was validated against nutritional data from literature.

Results and Discussion

Model refinements

Estimating the digestion-assimilation parameters

Parameter values for the digestion-assimilation module were estimated using literature data, while core DEB parameters remained constant. Data availability, however, varies among the species.

The most complete datasets were available for trout, which included gastric evacuation for different sizes (ranging between 5g and 71g) and temperatures (5°C, 10°C, and 15°C) (Figure 1), stomach volume at fish weight, as well as data on the relationship between water content and dry mass content in the stomach (Figure 2) and weight increase during a digestibility trial (Figure 3). Figures 4 and 5 illustrate the datasets used to estimate the digestion-assimilation parameters along with the predictions for Atlantic salmon. The data include gastric evacuation for different sizes and temperatures (Figure 4), as well as data on the relationship between stomach volume and fish weight increase during a digestibility trial (Figure 5). Figures 6 and 7 illustrate the datasets used to estimate the digestion-assimilation parameters along with the predictions for gilthead seabream and E. sea bass, respectively. The data include gastric evacuation and fish weight increase during a digestibility trial. Measurement of stomach volume were not available for both seabream and sea bass. Since this information is essential for estimating the digestibility parameters, data from related species were used as a substitute. Stomach capacity measurements were obtained from Gosch *et al.*, (2009) for species including white bass, bluegill, black crappie, spotted bass, and white crappie.

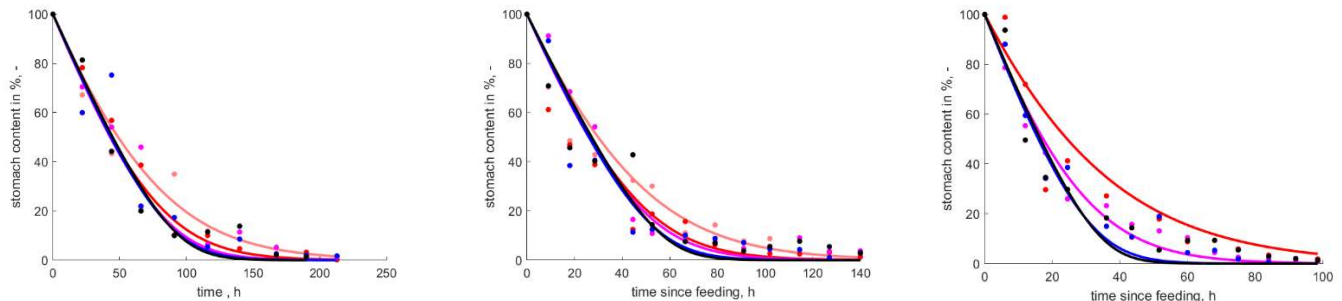


Figure 1. Species: Rainbow trout. The stomach content as % of the initial amount ingested is plotted over time for three different temperatures (Left: $T=5^{\circ}\text{C}$, Middle: $T=10^{\circ}\text{C}$; Right: $T=15^{\circ}\text{C}$), with fish fed *ad libitum* and time $t=0$ marking the cessation of feeding. Observations are represented by points, while model predictions are depicted by lines. The different colours in the plot indicate fish of varying sizes, with red representing smaller fish and black larger fish. Data on gastric evacuation were obtained from From and Rasmussen (1984).

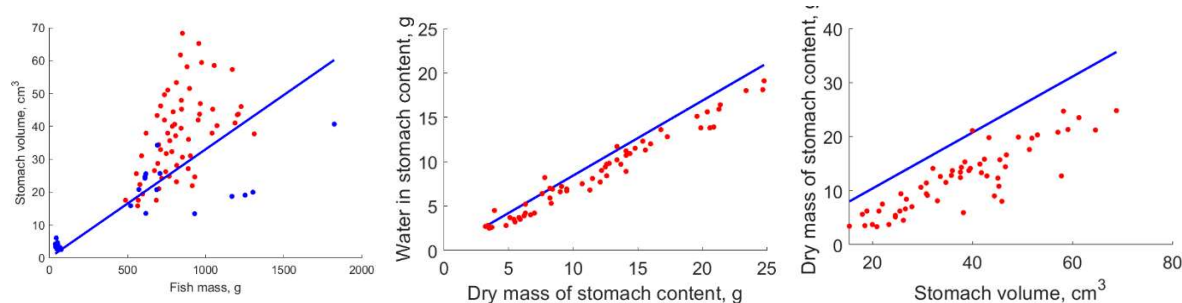


Figure 2. Species: Rainbow trout. Relationship between stomach volume and fish size (left) water in stomach content and stomach content dry mass (middle), and stomach content dry mass and stomach volume (right). Points indicate observations and lines model predictions. Data from Pirhonen and Koskela (2005) (red dots) and Ruohonen and Grove (1996) (blue dots).

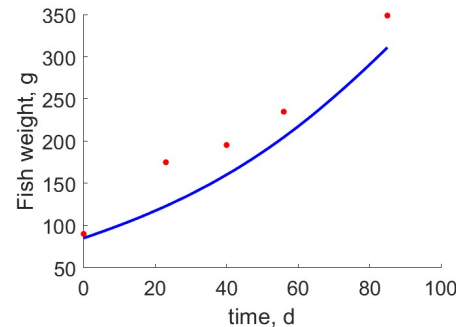


Figure 3. Species: Rainbow trout. Weight increase of rainbow trout during a 90-day digestibility trial (points) compared to model predictions (line). Data from Zhu et al. (2001)

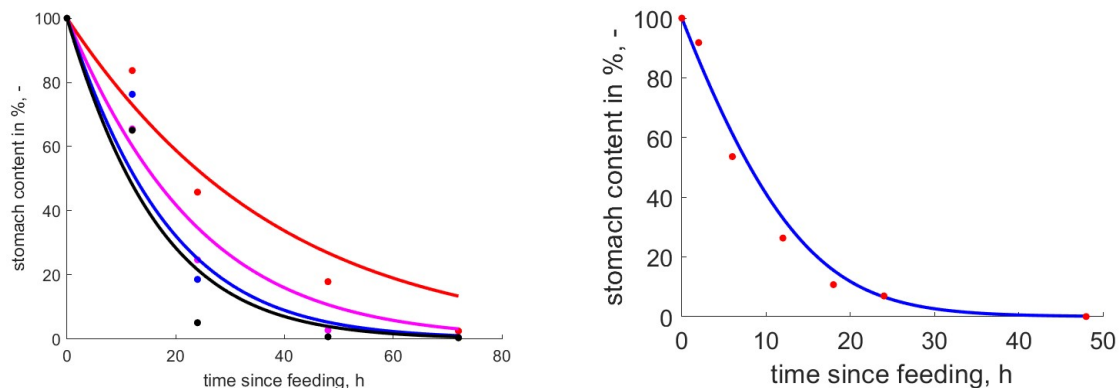


Figure 4. Species: Atlantic salmon. The stomach content as % of the initial amount ingested is plotted over time. Observations are represented by points, while model predictions are depicted by lines. Left: $T=6^\circ\text{C}$ and $W=154\text{g}$ (red), $T=10^\circ\text{C}$ and $W=263\text{g}$ (magenta), $T=14^\circ\text{C}$ and $W=296\text{g}$ (blue), $T=18^\circ\text{C}$ and $W=251\text{g}$ (black). Data from Handeland (2008). Right: $T=13.5^\circ\text{C}$ and $W=1131\text{g}$. Data from Aas et al. (2017).

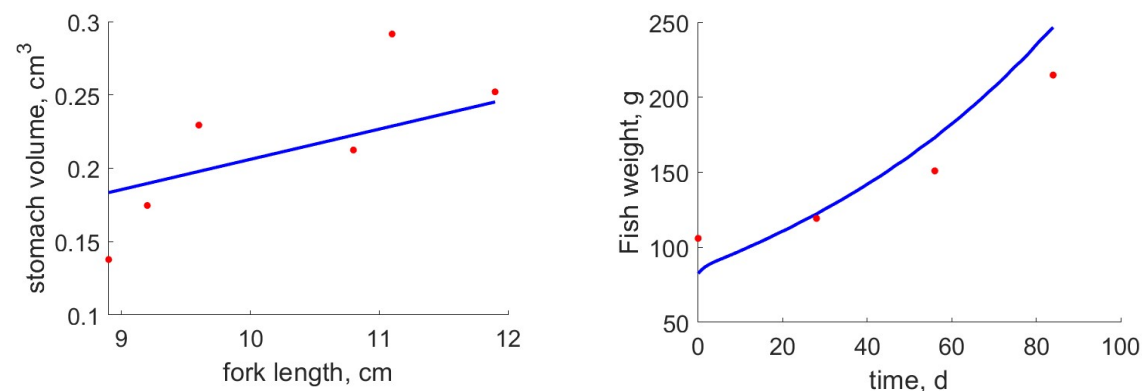


Figure 5. Species: Atlantic salmon. Relationship between stomach volume and fish size (left) and weight increase over 12 weeks of digestibility trial. Data from Cunjak (1992) and Villasante et al. (2022).

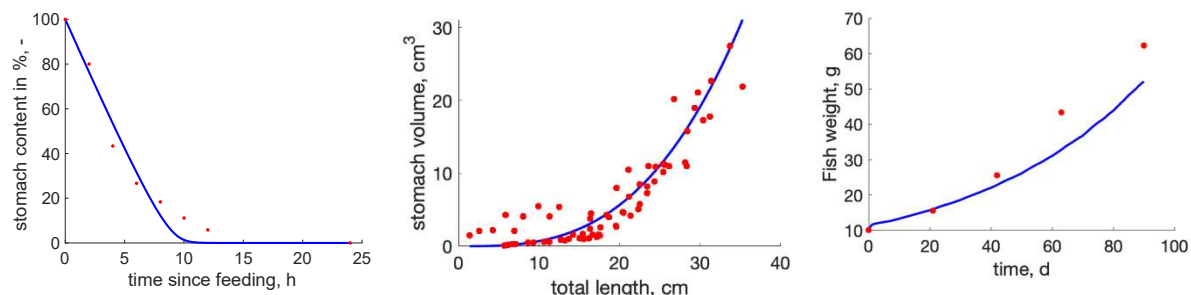


Figure 6. Species: Gilthead seabream. Left: stomach content as % of the initial amount ingested over time of fish of weight $W=150\text{g}$ at temperature $T=26^\circ\text{C}$ (Data from Nikolopoulou et al. (2011)). Middle: relationship between stomach volume and fish size (Data from Gosch et al. (2009)). Right: weight increase over 90 days of digestibility trial (Data from Santinha et al. (1996)).

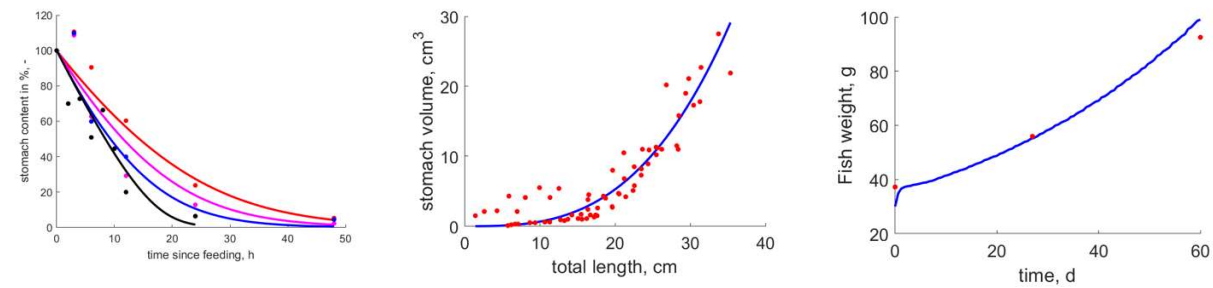


Figure 7. Species: European sea bass. Left: stomach content as % of the initial amount ingested over time ($T=15^\circ\text{C}$ and $W=26\text{g}$ (red), $T=20^\circ\text{C}$ and $W=26\text{g}$ (magenta), $T=25^\circ\text{C}$ and $W=26\text{g}$ (blue), $T=268^\circ\text{C}$ and $W=110\text{g}$ (black)) (Data from Santulli et al. (1993) and Nikolopoulou et al. (2011)). Middle: relationship between stomach volume and fish size (Data from Gosch et al. (2009)). Right: weight increase over 60 days of digestibility trial (Data from Gonçalves et al. (2019)).

The model accurately predicts the inverse relationship between temperature and gastric evacuation time (Figures 1, 4, 6 and 7), capturing the rate and duration of stomach emptying across a range of temperatures and fish sizes. The model generally supports the trend of larger fish emptying their stomachs faster. Stomach volume shows a positive relationship with fish size, with considerable scatter (Figures 2 and 5 (left) and Figures 6 and 7 (middle)).

Modeling the cost of swimming

The data used for the parametrization of the function for the metabolic cost of swimming and the results of the process are shown in Figures 8-11 for the different species. Respiration data at increasing speeds were obtained for a range of fish sizes and different temperatures, as depicted on the graphs. Model fitting was successful with a generally close match between observations and predictions. For all species, the swimming cost function was able to capture the upward-curving trajectory in respiration caused by increasing swimming speed despite the diverse nature of the datasets.

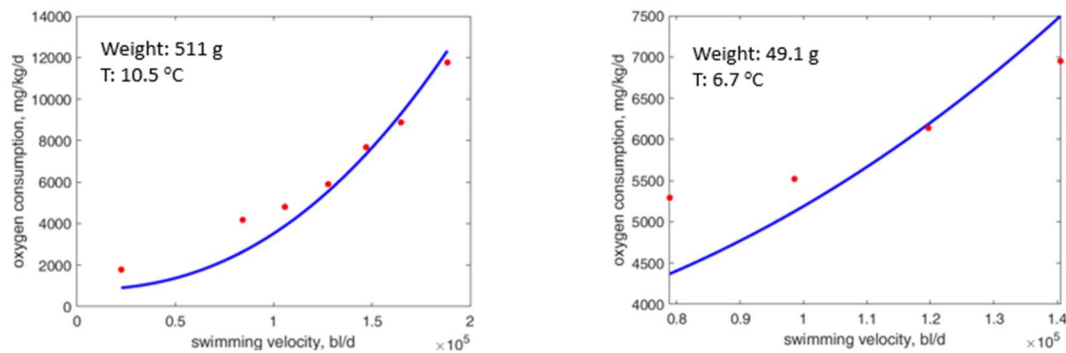


Figure 8. Oxygen consumption rate as a function of swimming speed for Atlantic salmon (*Salmo salar*). Points denote observations and lines model fitting. Data taken from Wilson et al. (2007) (left) and Castro et al. (2011) (right).

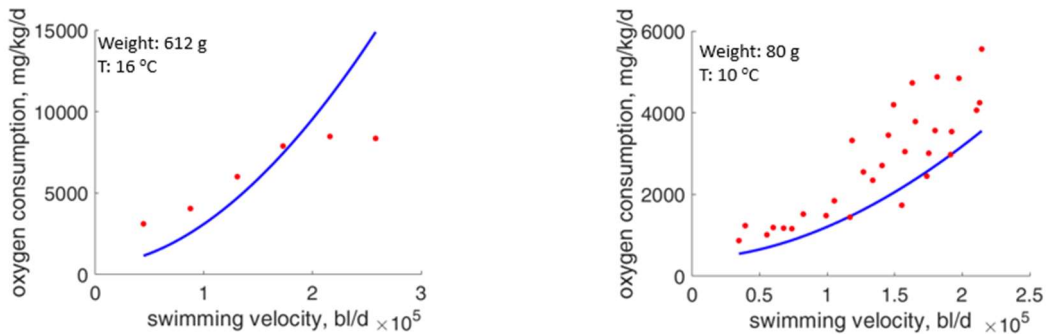


Figure 9. Oxygen consumption rate as a function of swimming speed for gilthead seabream (*Sparus aurata*). Points denote observations and lines model fitting. Data taken from Hachim et al. (2021) (left) and Svedsen et al. (2015) (right).

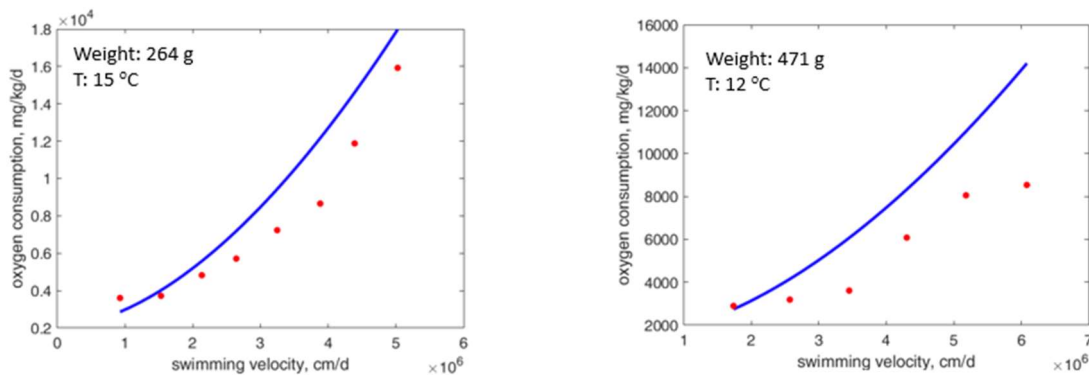


Figure 10. Oxygen consumption rate as a function of swimming speed for rainbow trout (*Oncorhynchus mykiss*). Points denote observations and lines model fitting. Data taken from Webb et al. (1971) (left) and Weatherley et al. (1982) (right).

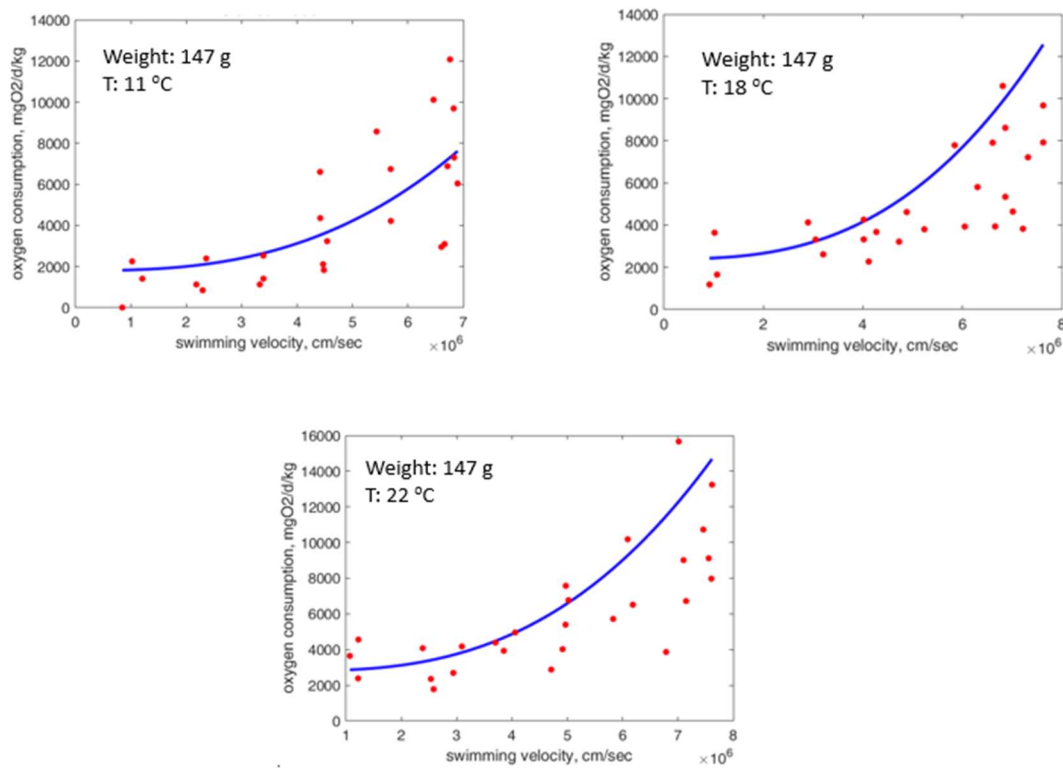


Figure 11. Oxygen consumption rate as a function of swimming speed for *E. sea bass* (*Dicentrarchus labrax*). Points denote observations and lines model fitting. Data taken from Claireaux et al. (2006) at different temperatures

Examples of model outputs

To showcase the AquaFishDEB model functionalities, examples of model outputs are provided in Figure 12. These examples serve to show the range of the variety of variables the model can predict and highlights some of the effects it is capable of capturing. Specifically, the simulation performed here demonstrates effects of feeding in terms of feeding level, composition, and schedule on a 10-d trial simulation on rainbow trout.

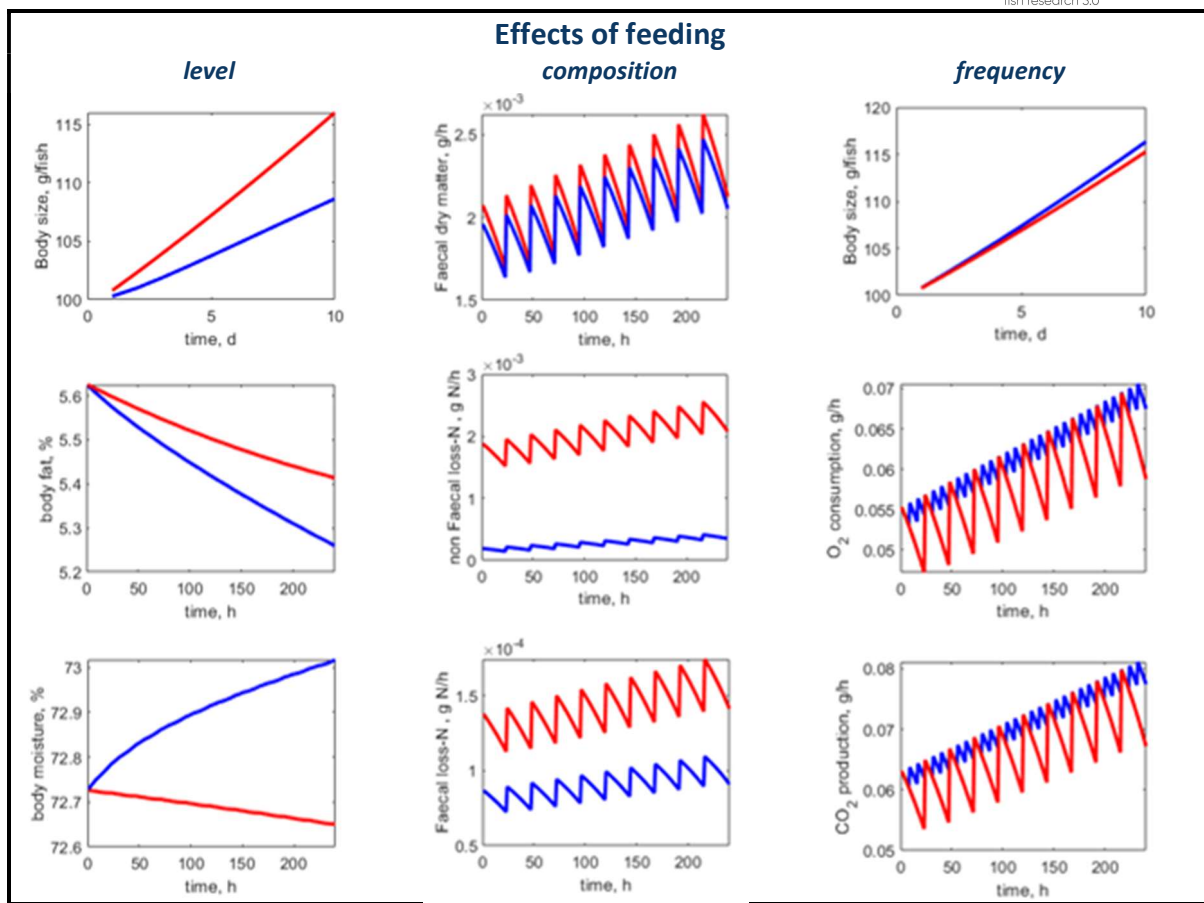


Figure 12. Model output examples. Simulations for a 10-day rainbow trout experiment under different feeding regimes. Left column: effects of feeding level (red: satiation feeding; blue: restricted feeding) on weight gain and body composition. Middle column: effects of feed composition (red: 45% protein, 20% fat, 15% carbohydrates; blue: 30% protein, 35% fat, 15% carbohydrates) on waste production such as solids and nitrogenous non-faecal and faecal loss. Right column: effect of feeding frequency (red: 1 meal/d; blue: 3 meals/day) on weight gain, oxygen consumption and carbon dioxide production.

Regarding the feeding level, it has strong effects on growth and body composition. As expected, feeding to satiation correlates with faster fish growth compared to restricted feeding. In addition, a higher feeding level results in a higher accumulation of fat and a decrease in moisture levels. With respect to effects of feed quality, the simulations show that diet composition results in substantial differences in waste production. Notably, simulating a high and a low protein diet caused large differences in the excretion of nitrogenous waste, both faecal and non-faecal, while the effect on the amount of solids produced was negligible. Finally, the model captures effects of the feeding schedule. Specifically, the frequency of feeding, whether it's a single meal per day or several meals per day plays a significant role in regulating the fluctuations of gaseous exchange. While feeding frequency itself hardly effects the growth of the fish or total waste production (not shown) it determines the oscillations of oxygen demand and carbon dioxide production throughout the day, namely, a higher feeding frequency tends to smooth out gaseous fluctuations.

Inclusion of new species

The parameter estimation for pikeperch resulted in an acceptable goodness of fit, quantified by the mean relative error (MRE = 0.208), giving an overall good match between predictions and observations. Comparison of the DEB model predictions against the observed data are given in Table 1 and Figures 13-14.

Table 1: Comparison of model predictions with observed data for pikeperch.

Symbol (unit)	Interpretation	T (°C)	Observations	Predictions	Source
a_b (d)	Age at birth	15	10.21	18.34	Güralp et al. (2017)
t_j (d)	Time since hatch at metamorphosis	19	26	18.82	Ostaszewska et al. (2008)
a_p (d)	Age at puberty female/ male	16	1460/1278	745.1/675.8	Aarts (2007)
a_m (d)	Life span	16	5840	6454	Aarts (2007)
L_p (cm)	Length at at puberty female/ male		40/35	42/38	Aarts (2007)
L_t (cm)	Ultimate total length		120	120.1	Aarts (2007)
W_w^b (g)	Wet weight at birth		$3.8 \cdot 10^{-4}$	$3.1 \cdot 10^{-4}$	Aarts (2007)
W_w^p (g)	Wet weight at puberty female/ male		741/496	772.8/608.4	Aarts (2007)
W_w^i (g)	Ultimate wet weight		$2 \cdot 10^4$	$1.81 \cdot 10^4$	Aarts (2007)

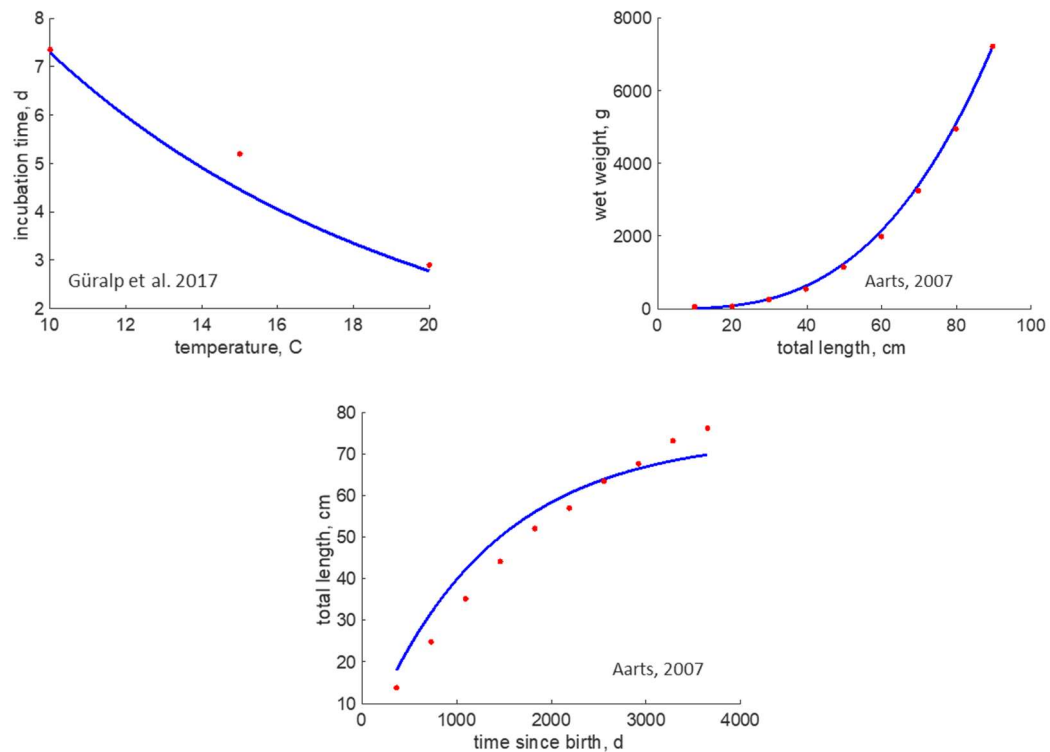


Figure 13. Fitting the pike perch DEB model to literature data, comparison of model predictions (lines) to observations (points): incubation time at different temperatures (Güralp et al., 2017), weight as a function of length (Aarts, 2007), length-at-time (Aarts, 2007).

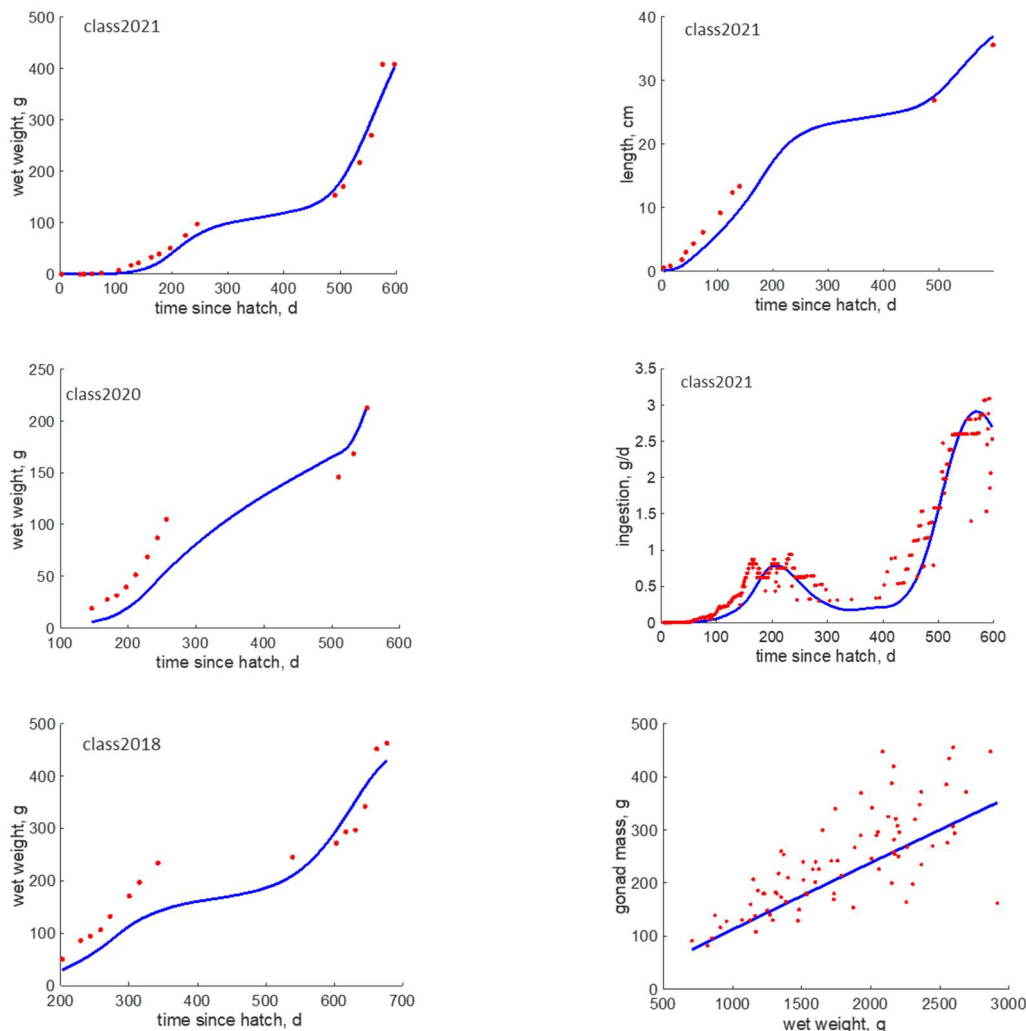


Figure 14 Fitting the pike perch DEB model to AE3.0 partner data (HAKI), comparison of model predictions (lines) to observations (points).

Regarding the validation of the *E. seabass* model, it was performed via comparison of model predictions to literature data on variables such as weight, oxygen consumption, carbon dioxide production and total ammonia nitrogen (TAN) excretion. The datasets included different fish sizes, temperatures, and diets that differed in quantity as well as quality. For each dataset, a simulation was run using as input the rearing conditions (temperature, trial duration, initial size, feed composition, ration size, and feeding schedule) of the respective study. Then, model predictions were plotted against the actual measurements while the line of equality ($y=x$) was also inserted for visualizing complete agreement between model predictions and observations (Figure 15). Overall, the results of this process showed a fairly accurate model. The model is able to capture the general patterns of the observations that were used, which is promising, especially given the diverse nature of the datasets that were used in terms of fish sizes, temperatures, diets, and experimental protocols. Particularly for growth and to a lesser extent for TAN, the validation points were scattered around the equality line indicating close match of predictions to observations. However, the model

tended to overestimate oxygen consumption. This bias appeared mainly under satiation feeding conditions (highlighted points) but was negligible for low feeding levels.

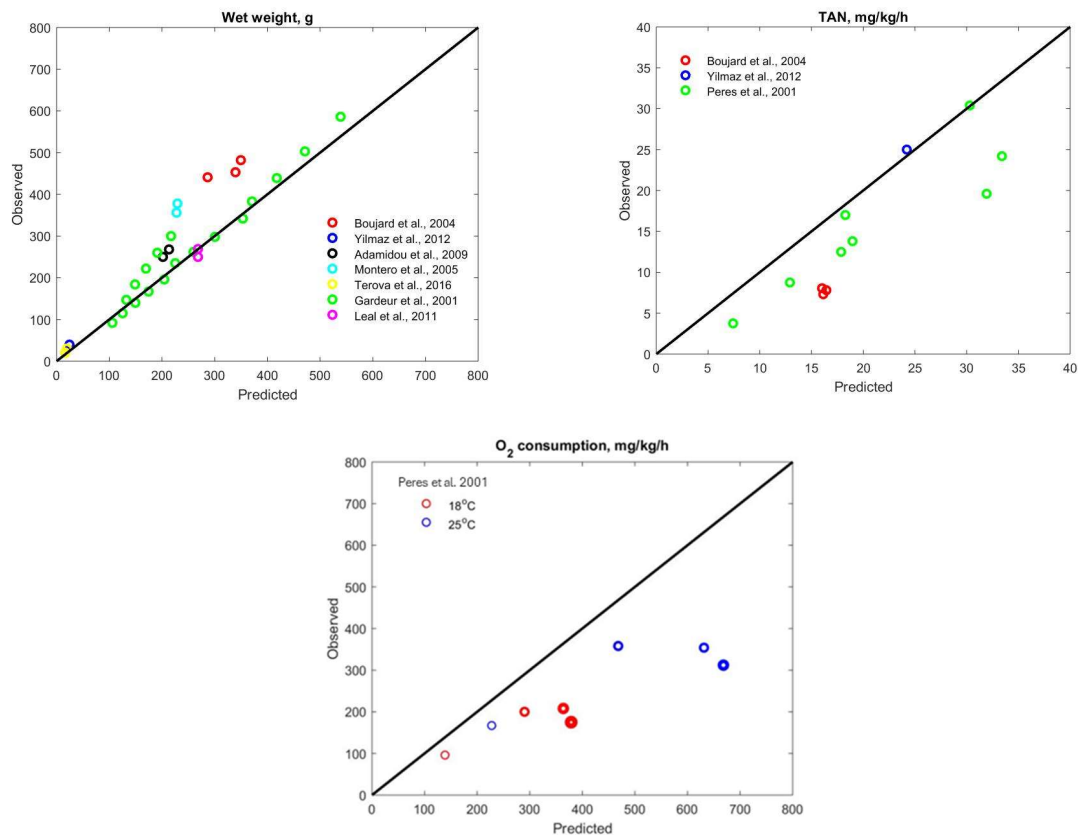


Figure 15 Model validation for *E. sea bass* (*Dicentrarchus labrax*). Observations vs. predictions, with line of equality.

Conclusion

In the course of AQUAEXCEL3.0, updates, improvements and new functionalities have been implemented in the AquafishDEB model. Namely, DEB models were developed for two new species, the *E. sea bass* and the pikeperch, and various refinements were implemented including the improvement of parameter estimates for the digestion module, the addition of predictions for body composition, and the incorporation of the effects of swimming speed on metabolism. The model captures the effects of the rearing environment with particular emphasis on aspects of nutrition and generates the model outputs relating to fish growth, feed consumption, waste production, body composition, and gaseous exchange that are required for the operation of the virtual laboratories and the establishment of interconnections with the other constituent models. This document, complements the code delivered as part of D4.6 by offering descriptions of the changes that have been implemented in the course of the project compared to previous version of the model.

Appendix

Model equations and parameters

Tables A1 and A2 give the equations of the AquaFishDEB model. Table A3 defines all model parameters and A4 provides the numerical values for the different species.

Table A1: State variables, energy fluxes and dynamics of the DEB model. Brackets [...] indicate quantities expressed per unit of structural volume and braces {} per unit of structural surface area.

State variables	
$V, L = V^{1/3}$	Structural body volume (cm^3), Volumetric structural length (cm)
$E, [E] = E / V$	Energy in reserve (J), Reserve density (J/cm^3)
E_H, E_R	Energy investment (J) into maturation, - to reproduction
M_X	Mass content of the food in the gut (mol)
Fluxes	
\dot{p}_A	Assimilation rate: $\dot{p}_A = \{\dot{p}_{Am}\} f L^2$, with $f_X = \frac{M_X}{M_X + M_K^X}$ and $M_K^X = \frac{\dot{J}_{EAm}}{\dot{J}_{Xgm}} \left((y_{EX_P} a_P)^{-1} + (y_{EX_{nP}} (1 - a_P))^{-1} - (y_{EX_P} a_P + y_{EX_{nP}} (1 - a_P))^{-1} \right)$
\dot{p}_C	Reserve mobilization rate: $L^3 [E] (\dot{v}/L - \dot{r})$ with $\dot{r} = \frac{\frac{\kappa [E] \dot{v}}{L} - \dot{p}_S}{[E_G] + [E] \kappa}$
\dot{p}_S	Somatic maintenance rate: $[\dot{p}_M] L^3$
\dot{p}_J	Maturity maintenance rate: $\dot{k}_J \min\{E_H, E_H^p\}$
\dot{p}_G	Growth rate: $\kappa \dot{p}_C - \dot{p}_S$
\dot{p}_R	Energy flux to maturation/reproduction: $(1 - \kappa) \dot{p}_C - \dot{p}_J$
\dot{p}_D	Dissipating power: $\dot{p}_S + \dot{p}_J + \dot{p}_R$ (larvae/juveniles); $\dot{p}_S + \dot{p}_J + (1 - \kappa_R) \dot{p}_R$ (adults)
Dynamics	
$\frac{d}{dt} V = \dot{r} V$	
$\frac{d}{dt} [E] = [\dot{p}_A] - [E] \dot{v}/L$	
$\frac{d}{dt} E_H = \dot{p}_R (E_H < E_H^p)$	
$\frac{d}{dt} E_R = \dot{p}_R (E_H \geq E_H^p)$	
$\frac{d}{dt} M_X = -(y_{XPE} + y_{XnP} + y_{PE}) \dot{p}_A / \mu_E$	

Table A2: Model equations that produce the output quantities. The equations use quantities defined in Table A1.

Wet weight (g)	$W = d_{VW} \left(V + (E + E_R) \frac{w_{Ed}}{d_{Ed} \mu_E} \right)$
Group size	$\frac{dN}{dt} = mN$, with m the mortality rate
Food consumed per meal (g)	$M_{Xi} = \min \left(w_X \frac{d_{XW}}{d_{Xd}} (M_{gm} - M_X), k_X W \right)$ with $M_{gm} = \left(y_{HX_d} \frac{d_{Xd}}{d_H} + 1 \right)^{-1} \frac{d_{Xd}}{w_X} \delta_g$
Feeding rate (g/d)	$\dot{J}_X = n M_{Xi}$, where n number of meals per day
Feed conversion ratio	$FCR = \frac{\dot{J}_X}{dW/dt}$
Faeces production (g/d)	$\dot{J}_P = \frac{y_{PE}}{\mu_E} \dot{p}_A$

Faecal loss-N (g/d)	$\dot{J}_{PN} = 14n_{NP} \frac{y_{PE}}{\mu_E} \dot{p}_A$
Non faecal loss-N	$\dot{J}_N = \eta_{ND} \dot{p}_D + \eta_{NG} \dot{p}_G$
Oxygen consumption	$\dot{J}_O = \eta_{OA} \dot{p}_A + \eta_{OD} \dot{p}_D + \eta_{OG} \dot{p}_G$
Carbon dioxide production	$\dot{J}_C = \eta_{CA} \dot{p}_A + \eta_{CD} \dot{p}_D + \eta_{CG} \dot{p}_G$

Table A3: Description of all parameters in the AquaFishDEB model.

Symbol	Units	Interpretation
$\{\dot{p}_{A_m}\}$	J/cm ² .d	Surface-specific max assimilation rate
\dot{v}	cm/d	Energy conductance
κ	-	Allocation fraction to soma
$\kappa_{X_P}, \kappa_{X_{nP}}, \kappa_{X_{Ch}}$	-	Digestion efficiency of protein, lipid and carbohydrates to reserves
κ_X	-	Digestion efficiency of food to reserves
κ_P	-	Faecation efficiency of food to faeces
κ_R	-	Reproduction efficiency
$[\dot{p}_M]$	J/cm ³ .d	Volume-specific somatic maintenance rate
$[E_G]$	J/cm ³	Specific costs for structure
E_H^b, E_H^j, E_H^p	J	Maturity threshold at birth, metamorphosis, puberty
k_J	1/d	Maturity maintenance rate coefficient
μ_*	J/mol	chemical potentials of * = X(food), P(product), V(structure), E(reserves)
w_*	g/mol	molecular weights of *
d_*	g/cm ³	specific density of *
$n_{C*}, n_{H*}, n_{O*}, n_{N*}$	-	chemical index of elements (C,H,O,N) in organic compounds *
auxiliary parameters		
T_A	K	Arrhenius temperature
δ_g	-	Gut-volume shape coefficient
$\{j_{EA_m}^d\}$	mol/cm ² .d	Surface-specific max assimilation rate
$\{\dot{p}_{A_m}\} = \mu_E \{j_{EA_m}^d\}$	J/cm ² d	Surface-specific max assimilation rate
$\{j_{Xg_m}\}$	1/cm ² .d	Surface-specific max digestion rate
a_P	-	Fraction of protein in food
$[M_{gm}]$ $= \left(y_{HX_d} \frac{d_{Xd}}{d_H} + 1 \right)^{-1} \frac{d_{Xd}}{w_X} \delta_g$	mol/cm ³	Volume-specific max capacity of the gut (dry weight)
$\kappa_{X_{nP}} = \kappa_{X_L} a_L + \kappa_{X_{NFE}} (1 - a_L)$	-	Digestion efficiency of non-protein to reserves, with a_L the fraction of lipids in the non-protein part of food
$y_{EX_P} = \kappa_{X_P} w_{X_P} / w_E$	mol P/mol E	yield of reserve on protein
$y_{EX_{nP}} = \kappa_{X_{nP}} w_{X_{nP}} / w_E$	mol nP/mol E	yield of reserve on the non-protein
$\kappa_X = \theta_P \kappa_{X_P} + \theta_L \kappa_{X_L} + \theta_A \kappa_{X_A} + \theta_{Ch} \kappa_{X_{Ch}}$	-	Digestion efficiency of food to reserves, where θ are the fractions of protein, lipid, ash, and carbohydrates in food and κ their respective digestibilities.
$\kappa_P = \theta_P (1 - \kappa_{X_P}) + \theta_L (1 - \kappa_{X_L}) + \theta_A (1 - \kappa_{X_A}) + \theta_{Ch} (1 - \kappa_{X_{Ch}})$	-	Digestion efficiency of food to faeces, where θ are the fractions of protein, lipid, ash, and carbohydrates in food and κ their respective digestibilities.
$y_{PE} = \frac{\kappa_P \mu_E}{\kappa_X \mu_P}$	-	yield of faeces on reserve
k_X	-	Food as fraction of body (wet) weight
y_{HX_d}	-	g of water absorbed per g of dry food ingested
$\{\dot{p}_L\}$	J/cm ² .d	Surface-specific cost for locomotion
$\theta_{PrV}, \theta_{PrE}$	-	Fraction of protein in dry structure and reserve

Table A4. Numerical values for the main *AquaFishDEB* parameters for the five species. Compound and food-specific parameters are excluded.

Symbol	Atlantic salmon	Gilthead seabream	Rainbow trout	E. sea bass	Pikeperch
$\{\dot{p}_{A_m}\}$	170.77	29.49	8234	64.32	521.53
\dot{v}	$29 \cdot 10^{-3}$	$38 \cdot 10^{-3}$	$32 \cdot 10^{-3}$	$34 \cdot 10^{-3}$	$7 \cdot 10^{-3}$
κ	0.94	0.97	0.62	0.72	0.77
κ_R	0.95	0.95	0.95	0.95	0.95
$[\dot{p}_M]$	52.11	66.38	343.88	20.65	159.67
$[E_G]$	5230	5234.23	5267.56	5230	5200
E_H^b, E_H^j, E_H^p	15.01, $2.4 \cdot 10^4$, $2.6 \cdot 10^5$	$2.4 \cdot 10^{-2}$, 212.8, $3.8 \cdot 10^5$	43.29, 854.1, $3.9 \cdot 10^6$	0.78, 317.3, $1.3 \cdot 10^6$	$29 \cdot 10^{-3}$, 1.99, $1.1 \cdot 10^5$
\dot{k}_J	0.002	0.002	0.002	0.002	0.002
T_A	3804	8000	8000	3689	8000
δ_g	0.12	0.15	0.59	0.14	-
$\{\dot{J}_{EA_m}^d\}$	$47 \cdot 10^{-4}$	$88 \cdot 10^{-5}$	$42.9 \cdot 10^{-4}$	$11.28 \cdot 10^{-4}$	-
$\{\dot{J}_{Xg_m}\}$	$10.8 \cdot 10^{-3}$	$79 \cdot 10^{-3}$	1828	0.11	-
y_{HX_d}	$92 \cdot 10^{-3}$	$92 \cdot 10^{-3}$	$84.25 \cdot 10^{-2}$	$92 \cdot 10^{-3}$	-
$\{\dot{p}_L\}$	$7.95 \cdot 10^{-11}$	$1.69 \cdot 10^{-10}$	$6.24 \cdot 10^{-10}$	$1.93 \cdot 10^{-11}$	-
$\theta_{PrV}, \theta_{PrE}$	0.73, 0.69	0.55, 0.65	0.89, 0.68	0.78, 0.62	-

References

Aarts, T.W.P.M., 2007. Kennisdocument snoekbaars, Sander lucioperca (Linnaeus,1758). Kennisdocument 16. Sportvisserij Nederland, Bilthoven.

Aas, T.S., Sixten, H.J., Hillestad, M., Sveier, H., Ytrestøyl, T., Hatlen, B., Åsgård, T., 2017. Measurement of gastrointestinal passage rate in Atlantic salmon (*Salmo salar*) fed dry or soaked feed. *Aquaculture Reports* 8, 49–57. <https://doi.org/10.1016/j.aqrep.2017.10.001>

Adamidou, S., Nengas, I., Alexis, M., Fountoulaki, E., Nikolopoulou, D., Campbell, P., Karacostas, I., Bell, J.G.B., Jauncey, K., 2009. Apparent nutrient digestibility and gastrointestinal evacuation time in European seabass (*Dicentrarchus labrax*) fed diets containing different levels of legumes. *Aquaculture* 289, 106–112. <https://doi.org/10.1016/j.aquaculture.2009.01.015>

Boujard, T., Gélineau, A., Covès, D., Corraze, G., Dutto, G., Gasset, E., Kaushik, S., 2004. Regulation of feed intake, growth, nutrient and energy utilisation in European sea bass (*Dicentrarchus labrax*) fed high fat diets. *Aquaculture* 231, 529–545. <https://doi.org/10.1016/j.aquaculture.2003.11.010>

Breck, J.E., 2014. Body composition in fishes: body size matters. *Aquaculture* 433, 40–49. <https://doi.org/10.1016/j.aquaculture.2014.05.049>

Castro, V., Grisdale-Helland, B., Helland, S.J., Kristensen, T., Jørgensen, S.M., Helgerud, J., Claireaux, G., Farrell, A.P., Krasnov, A., Takle, H., 2011. Aerobic training stimulates growth and promotes disease resistance in Atlantic salmon (*Salmo salar*). *Comparative Biochemistry and Physiology Part A: Molecular & Integrative Physiology* 160, 278–290. <https://doi.org/10.1016/j.cbpa.2011.06.013>

Cerdá, J., Carrillo, M., Zanuy, S., Ramos, J., de la Higuera, M., 1994. Influence of nutritional composition of diet on sea bass, *Dicentrarchus labrax* L., reproductive performance and egg and larval quality. *Aquaculture* 128, 345–361. [https://doi.org/10.1016/0044-8486\(94\)90322-0](https://doi.org/10.1016/0044-8486(94)90322-0)

Claireaux, G., Couturier, C., Groison, A.-L., 2006. Effect of temperature on maximum swimming speed and cost of transport in juvenile European sea bass (*Dicentrarchus labrax*). *Journal of Experimental Biology* 209, 3420–3428. <https://doi.org/10.1242/jeb.02346>

Cunjak, R.A., 1992. Comparative feeding, growth and movements of Atlantic salmon (*Salmo salar*) parr from riverine and estuarine environments. *Ecology of Freshwater Fish* 1, 26–34. <https://doi.org/10.1111/j.1600-0633.1992.tb00004.x>

Fernández-Palacios, H., Izquierdo, M., Robaina, L., Valencia, A., Salhi, M., Montero, D., 1997. The effect of dietary protein and lipid from squid and fish meals on egg quality of broodstock for gilthead seabream (*Sparus aurata*). *Aquaculture* 148, 233–246. [https://doi.org/10.1016/S0044-8486\(96\)01312-9](https://doi.org/10.1016/S0044-8486(96)01312-9)

Føre, M., Alver, M., Alfredsen, J.A., Marafioti, G., Senneset, G., Birkevold, J., Willumsen, F.V., Lange, G., Espmark, Å., Terjesen, B.F., 2016. Modelling growth performance and feeding behaviour of Atlantic salmon (*Salmo salar* L.) in commercial-size aquaculture net pens: Model details and validation through full-scale experiments. *Aquaculture* 464, 268–278. <https://doi.org/10.1016/j.aquaculture.2016.06.045>

From, J., Rasmussen, G., 1984. A growth model, gastric evacuation, and body composition in rainbow trout *Salmo Gairdneri* Richardson, 1836. *Dana* 3, 61–139.

Güralp, H., Pocherniaieva, K., Blecha, M., Policar, T., Pšenička, M., Saito, T., 2017. Development, and effect of water temperature on development rate, of pikeperch *Sander lucioperca* embryos. *Theriogenology* 104, 94–104. <https://doi.org/10.1016/j.theriogenology.2017.07.050>

Gonçalves, R.A., Serradeiro, R., Machado, M., Costas, B., Hunger, C., Dias, J., 2019. Interactive effects of dietary fishmeal level and plant essential oils supplementation on European sea bass, *Dicentrarchus labrax*: Growth performance, nutrient utilization, and immunological response. *Journal of the World Aquaculture Society* 50, 1078–1092

Gosch, N.J.C., Pope, K.L., Michaletz, P.H., 2009. Stomach Capacities of Six Freshwater Fishes. *Journal of Freshwater Ecology* 24, 645–649. <https://doi.org/10.1080/02705060.2009.9664342>

Hachim, M., Rouyer, T., Dutto, G., Kerzerho, V., Bernard, S., Bourjea, J., McKenzie, D.J., 2021. Oxygen uptake, heart rate and activities of locomotor muscles during a critical swimming speed protocol in the gilthead sea bream *Sparus aurata*. *Journal of Fish Biology* 98, 886–890. <https://doi.org/10.1111/jfb.14621>

Hejlesen, R., Scheffler, F.B., Byrge, C.G., Kjær-Sørensen, K., Oxvig, C., Fago, A., Malte, H., 2024. Assessing metabolic rates in zebrafish using a 3D-printed intermittent-flow respirometer and swim tunnel system. *Biology Open* 13, bio060375. <https://doi.org/10.1242/bio.060375>

Helander, H.F., Fändriks, L., 2014. Surface area of the digestive tract – revisited. *Scandinavian Journal of Gastroenterology* 49, 681–689. <https://doi.org/10.3109/00365521.2014.898326>

Hvas, M., Oppedal, F., 2019. Influence of experimental set-up and methodology for measurements of metabolic rates and critical swimming speed in Atlantic salmon *Salmo salar*. *Journal of Fish Biology* 95, 893–902. <https://doi.org/10.1111/jfb.14087>

Kooijman, S.A.L.M., 2010. *Dynamic Energy Budget Theory for Metabolic Organisation*. Cambridge University Press.

Leal, E., Fernández-Durán, B., Guillot, R., Ríos, D., Cerdá-Reverter, J.M., 2011. Stress-induced effects on feeding behavior and growth performance of the sea bass (<Emphasis Type="Italic">*Dicentrarchus labrax*</Emphasis>): a self-feeding approach. *J Comp Physiol B* 181, 1035–1044. <https://doi.org/10.1007/s00360-011-0585-z>

Lika, K., Stavrakidis-Zachou, O., Papandroulakis, N. 2020. Final model for growth, feed consumption and waste production simulation, AQUAEXCEL2020, D5.6.

Marques, G.M., Lika, K., Augustine, S., Pecquerie, L., Kooijman, S.A.L.M., 2019. Fitting multiple models to multiple data sets. *Journal of Sea Research* 143, 48–56. <https://doi.org/10.1016/j.seares.2018.07.004>

Montero, D., Robaina, L., Caballero, M.J., Ginés, R., Izquierdo, M.S., 2005. Growth, feed utilization and flesh quality of European sea bass (*Dicentrarchus labrax*) fed diets containing vegetable oils: A time-course study on the effect of a re-feeding period with a 100% fish oil diet. *Aquaculture, Fish Nutrition and Feeding* 248, 121–134. <https://doi.org/10.1016/j.aquaculture.2005.03.003>

Nikolopoulou, D., Moutou, K.A., Fountoulaki, E., Venou, B., Adamidou, S., Alexis, M.N., 2011. Patterns of gastric evacuation, digesta characteristics and pH changes along the gastrointestinal tract of gilthead sea bream (*Sparus aurata* L.) and European sea bass (*Dicentrarchus labrax* L.). *Comparative Biochemistry and Physiology Part A: Molecular & Integrative Physiology* 158, 406–414. <https://doi.org/10.1016/j.cbpa.2010.11.021>

Ohlberger, J., Staaks, G., Hölker, F., 2006. Swimming efficiency and the influence of morphology on swimming costs in fishes. *J Comp Physiol B* 176, 17–25. <https://doi.org/10.1007/s00360-005-0024-0>

Ostaszewska T. and Dabrowski K. and Wegner A. and Krawiec M., 2008. The effects of feeding on muscle growth dynamics and the proliferation of myogenic progenitor cells during pike perch development (*Sander lucioperca*). *Journal of the World Aquaculture Society* 39, 184 – 195.

Pecquerie, L., Petitgas, P., Kooijman, S.A.L.M., 2009. Modeling fish growth and reproduction in the context of the Dynamic Energy Budget theory to predict environmental impact on anchovy spawning duration. *Journal of Sea Research, Metabolic organization: 30 years of DEB applications and developments* 62, 93–105. <https://doi.org/10.1016/j.seares.2009.06.002>

Peres, H., Oliva-Teles, A., 2001. Effect of dietary protein and lipid level on metabolic utilization of diets by european sea bass (*Dicentrarchus labrax*) juveniles. *Fish Physiology and Biochemistry* 25, 269–275. <https://doi.org/10.1023/A:1023239819048>

Pirhonen, J., Koskela, J., 2005. Indirect estimation of stomach volume of rainbow trout *Oncorhynchus mykiss* (Walbaum). *Aquaculture Research* 36, 851–856. <https://doi.org/10.1111/j.1365-2109.2005.01293.x>

Pörtner, H.-O., Bock, C., Mark, F.C., 2017. Oxygen- and capacity-limited thermal tolerance: bridging ecology and physiology. *Journal of Experimental Biology* 220, 2685–2696. <https://doi.org/10.1242/jeb.134585>

Rennie, S., Huntingford, F.A., Loeland, A.-L., Rimbach, M., 2005. Long term partial replacement of dietary fish oil with rapeseed oil; effects on egg quality of Atlantic salmon *Salmo salar*. *Aquaculture, Fish Nutrition and Feeding* 248, 135–146. <https://doi.org/10.1016/j.aquaculture.2005.03.015>

Ruohonen, K., Grove, D.J., 1996. Gastrointestinal responses of rainbow trout to dry pellet and low-fat herring diets. Journal of Fish Biology 49, 501–513.
<https://doi.org/10.1111/j.1095-8649.1996.tb00045.x>

Sadoul, B., Augustine, S., Zimmer, E., Bégout, M.-L., Vijayan, M.M., 2019. Prediction of long-term variation in offspring metabolism due to BPA in eggs in rainbow trout using the DEB model. *Journal of Sea Research* 143, 222–230. <https://doi.org/10.1016/j.seares.2018.05.011>

Santull, A., Modica, A., Cusenza, L., Curatolo, A., D'Amelio, V., 1993. Effects of temperature on gastric evacuation rate and absorption and transport of dietary lipids in sea bass (*Dicentrarchus labrax*, L.). *Comparative Biochemistry and Physiology Part A: Physiology* 105, 363–367. [https://doi.org/10.1016/0300-9629\(93\)90222-P](https://doi.org/10.1016/0300-9629(93)90222-P)

Santinha, P. j. m., Gomes, E. f. s., Coimbra, J. o., 1996. Effects of protein level of the diet on digestibility and growth of gilthead sea bream, *Sparus auratus* L. *Aquaculture Nutrition* 2, 81–87. <https://doi.org/10.1111/j.1365-2095.1996.tb00012.x>

Sarà, G., Gouhier, T.C., Brigolin, D., Porporato, E.M.D., Mangano, M.C., Mirto, S., Mazzola, A., Pastres, R., 2018. Predicting shifting sustainability trade-offs in marine finfish aquaculture under climate change. *Global Change Biology* 24, 3654–3665. <https://doi.org/10.1111/gcb.14296>

Serpa, D., Ferreira, P.P., Ferreira, H., da Fonseca, L.C., Dinis, M.T., Duarte, P., 2013. Modelling the growth of white seabream (*Diplodus sargus*) and gilthead seabream (*Sparus aurata*) in semi-intensive earth production ponds using the Dynamic Energy Budget approach. *Journal of Sea Research* 76, 135–145. <https://doi.org/10.1016/j.seares.2012.08.003>

Silva, T.S. de C., Santos, L.D. dos, Silva, L.C.R. da, Michelato, M., Furuya, V.R.B., Furuya, W.M., 2015. Length-weight relationship and prediction equations of body composition for growing-finishing cage-farmed Nile tilapia. *R. Bras. Zootec.* 44, 133–137. <https://doi.org/10.1590/S1806-92902015000400001>

Stavrakidis-Zachou, O., Papandroulakis, N., Lika, K., 2019. A DEB model for European sea bass (*Dicentrarchus labrax*): Parameterisation and application in aquaculture. *Journal of Sea Research, Ecosystem based management and the biosphere: a new phase in DEB research* 143, 262–271. <https://doi.org/10.1016/j.seares.2018.05.008>

Svendsen, J.C., Tirsgaard, B., Cordero, G.A., Steffensen, J.F., 2015. Intraspecific variation in aerobic and anaerobic locomotion: gilthead sea bream (*Sparus aurata*) and Trinidadian guppy (*Poecilia reticulata*) do not exhibit a trade-off between maximum sustained swimming speed and minimum cost of transport. *Front. Physiol.* 6. <https://doi.org/10.3389/fphys.2015.00043>

Terova, G., Díaz, N., Rimoldi, S., Ceccotti, C., Gliozheni, E., Piferrer, F., 2016. Effects of Sodium Butyrate Treatment on Histone Modifications and the Expression of Genes Related to Epigenetic Regulatory Mechanisms and Immune Response in European Sea Bass (*Dicentrarchus Labrax*) Fed a Plant-Based Diet. *PLoS One* 11, e0160332. <https://doi.org/10.1371/journal.pone.0160332>

Villasante, A., Ramírez, C., Rodríguez, H., Dantagnan, P., Hernández, A., Figueroa, E., Romero, J., 2022. Dietary carbohydrate-to-protein ratio influences growth performance, hepatic health and dynamic of gut microbiota in atlantic salmon (*Salmo salar*). *Animal Nutrition* 10, 261–279. <https://doi.org/10.1016/j.aninu.2022.04.003>

Yilmaz, S., Sebahattin, E., Celik, E. 2012. Effects of herbal supplements on growth performance of sea bass (*Dicentrarchus labrax*): Change in body composition and some blood parameters. *Energy*, 5, 21-66.

Washburn, B.S., Frye, D.J., Hung, S.S.O., Doroshov, S.I., Conte, F.S., 1990. Dietary effects on tissue composition, oogenesis and the reproductive performance of female rainbow trout (*Oncorhynchus mykiss*). *Aquaculture* 90, 179–195. [https://doi.org/10.1016/0044-8486\(90\)90340-S](https://doi.org/10.1016/0044-8486(90)90340-S)

Weatherley, A.H., Rogers, S.C., Pincock, D.G., Patch, J.R., 1982. Oxygen consumption of active rainbow trout, *Salmo gairdneri* Richardson, derived from electromyograms obtained by radiotelemetry. *Journal of Fish Biology* 20, 479–489. <https://doi.org/10.1111/j.1095-8649.1982.tb03941.x>

Webb, P.W., 1971. The Swimming Energetics of Trout: I. Thrust and Power Output at Cruising Speeds. *Journal of Experimental Biology* 55, 489–520. <https://doi.org/10.1242/jeb.55.2.489>

Wilson, C.M., Friesen, E.N., Higgs, D.A., Farrell, A.P., 2007. The effect of dietary lipid and protein source on the swimming performance, recovery ability and oxygen consumption of Atlantic salmon (*Salmo salar*). *Aquaculture* 273, 687–699. <https://doi.org/10.1016/j.aquaculture.2007.10.027>

Zhu, S., Chen, S., Hardy, R.W., Barrows, F.T., 2001. Digestibility, growth and excretion response of rainbow trout (*Oncorhynchus mykiss* Walbaum) to feeds of different ingredient particle sizes. *Aquaculture Research* 32, 885–893. <https://doi.org/10.1046/j.1365-2109.2001.00624.x>

Document Information

EU Project	No 871108	Acronym	AQUAEXCEL3.0
Full Title	AQUAculture infrastructures for EXCELlence in European fish research 3.0		
Project website	www.aquaexcel.eu		

Deliverable	N°	4.6	Title	Final models for growth
Work Package	N°	4	Title	Technological tools for improved experimental procedures
Work Package Leader	Finn Olav Bjørnson			
Work Participants	HCMR, INRAPEIMA, NTNU, SINTEF, NAIK, NOFIMA			

Lead Beneficiary	HCMR
Authors	Konstadia Lika, University of Crete, lika@uoc.gr Orestis Starvakidis-Zachou, HCMR, ostavrak@hcmr.gr Nikos Papandroulakis, HCMR, npap@hcmr.gr
Reviewers	Chris Noble, NOFIMA, Chris.Noble@Nofima.no Finn Olav Bjørnson, SINTEF Ocean, finn.o.bjornson@sintef.no

Due date of deliverable	31.10.2024
Submission date	31.10.2024
Dissemination level	PU
Type of deliverable	Other

Version log			
Issue Date	Revision N°	Author	Change
04.10.2024	0.9	Orestis	First version
17.10.2024	1	Orestis	Updated with input from reviewers
31.10.2024	2	Orestis	Updated with input from second review